Elucidation of Pelareorep Pharmacodynamics in A Phase I Trial in Patients with *KRAS*-Mutated Colorectal Cancer

Sanjay Goel[1,2], Allyson J. Ocean[3], Ruwan Y. Parakrama[1], Mohammad H. Ghalib[1], Imran Chaudhary[1], Umang Shah[1], Sengottuvel Viswanathan[1], Himanshu Kharkwal[1], Matthew Coffey[4], and Radhashree Maitra[1,2]

ABSTRACT

KRAS mutation is a negative predictive biomarker of anti-EGFR agents in patients with metastatic colorectal cancer (mCRC), and remains an elusive target. Pelareorep, a double-stranded RNA virus selectively replicates in *KRAS*-mutated cells, and is synergistic with irinotecan. A dose escalation trial of FOLFIRI/bevacizumab [irinotecan (150–180 mg/m^2) and pelareorep (1×10^{10} $TCID_{50}$–3×10^{10} $TCID_{50}$)] was implemented in adult patients with oxaliplatin refractory/intolerant, *KRAS*-mutant mCRC. Pelareorep was administered intravenously over 1 hour on days 1–5 every 4 weeks. Additional studies included pharmacokinetics, tumor morphology, and immune responses. Among FOLFIRI-naïve patients, the highest dose of FOLFIRI/bevacizumab (180 mg/m^2 irinotecan) and pelareorep (3×10^{10} $TCID_{50}$) was well tolerated, without a dose-limiting toxicity. At the recommended phase II dose, 3 of 6 patients (50%) had a partial response; the median progression-free and overall survival (PFS, OS) were 65.6 weeks and 25.1 months, respectively. Toxicities included myelosuppression, fatigue, and diarrhea. Transmission electron microscopy revealed viral factories (viral collections forming vesicular structures), at various stages of development. Immunogold staining against viral capsid σ-1 protein demonstrated viral "homing" in the tumor cells. The nucleus displayed sufficient euchromatin regions suggestive of active transcription. Flow cytometry revealed rapid dendritic cell maturation (48 hours) with subsequent activation of cytotoxic T cells (7 days). The combination of pelareorep with FOLFIRI/bevacizumab is safe. The PFS and OS data are encouraging and deserve further exploration. Pelareorep leads to a clear recurrent immune stimulatory response with cytotoxic T-cell activation, and homes and replicates in the tumor.

Introduction

Colorectal cancer pathogenesis is marked by a series of somatic alterations, among which an oncogenic mutation in the *KRAS* gene (40%–45% of patients) is common and one of the best described (1, 2). The outlook for patients with metastatic colorectal cancer (mCRC) has seen dramatic improvements over the past 20 years. While 5-fluorouracil (5-FU) remained the only drug with any clinical benefit for 4 preceding decades, there are now 14 drugs that are FDA approved and in active use (3). The median overall survival (OS) has improved from a dismal 12 months to close to 30 months since the availability of these agents (4, 5). An essential arsenal in the struggle against this scourge remains the combination chemotherapy of folinic acid (FOL), infusion 5-FU (F), and irinotecan (IRI; FOLFIRI), frequently used as a second-line chemotherapy combination from among the chemotherapy armamentarium in patients with mCRC.

The presence of a *KRAS* mutation in a patient's tumor is now a well-accepted predictive biomarker of exclusion of EGFR-directed therapy in mCRC (1, 6). In patients with a *KRAS* wild-type (WT) tumor, both cetuximab and panitumumab offer valuable clinical benefit. In spite of tremendous investment, both financial and intellectual, over the past decades, targeting *KRAS* has remained an elusive goal (7, 8). In the 40%–45% of patients with mCRC with a *KRAS* mutation, treatment options are limited once they are refractory to oxaliplatin- and irinotecan-based regimens (5, 9, 10). There is therefore an urgent unmet need to develop novel interventions that can be made available as a meaningful part of the treatment paradigm.

Pelareorep (Reolysin, Oncolytics Biotech Inc.) is reovirus type 3 Dearing strain, a naturally occurring, ubiquitous, nonenveloped human double-stranded (ds) RNA virus. It is purported to replicate selectively in transformed cells with an EGFR pathway induction or *KRA*S mutation (11, 12), or with a v-erb B oncogene (13). In non-transformed cells, the early viral transcripts lead to the auto-phosphorylation of dsRNA-activated protein kinase R (PKR). The activated phosphorylated PKR in turn phosphorylates and activates the alpha subunit of the eukaryotic translation initiation factor 2 and subsequently inhibits viral protein synthesis (14). In transformed cells, the active Ras signaling pathway inhibits the auto-phosphorylation of PKR, and thereby permits the synthesis of viral proteins, facilitating the uninhibited replication of the pelareorep (15).

We have previously elucidated in *in vitro* models that pelareorep is selectively efficient in its cytotoxic effect in *KRAS*-mutant conditions, in contrast to *KRAS* WT, and is synergistic with irinotecan (12). We carried over these observations, and confirmed them in *in vivo* xenograft models of colorectal cancer cell lines. Subsequently, we launched a phase I dose escalation open-label clinical trial of pelareorep combined with standard FOLFIRI, and bevacizumab, in patients with *KRAS*-mutant oxaliplatin refractory/intolerant mCRC.

[1]Department of Medical Oncology, Montefiore Medical Center, Bronx, New York. [2]Albert Einstein College of Medicine, Bronx, New York. [3]Department of Medical Oncology, New York-Presbyterian/Weill Cornell Medical Center, New York, New York. [4]Oncolytics Inc., Calgary, Alberta, Canada.

Note: Supplementary data for this article are available at Molecular Cancer Therapeutics Online (http://mct.aacrjournals.org/).

Prior presentation: Presented in part at the European Society of Clinical Oncology Congress in 2018.

Corresponding Author: Sanjay Goel, Montefiore Medical Center, and Albert Einstein College of Medicine, 1695 Eastchester Road, Bronx, NY 10461. Phone: 718-405-8404; Fax: 718-405-8433; E-mail: sgoel@montefiore.org

Mol Cancer Ther 2020;19:1148–56

doi: 10.1158/1535-7163.MCT-19-1117

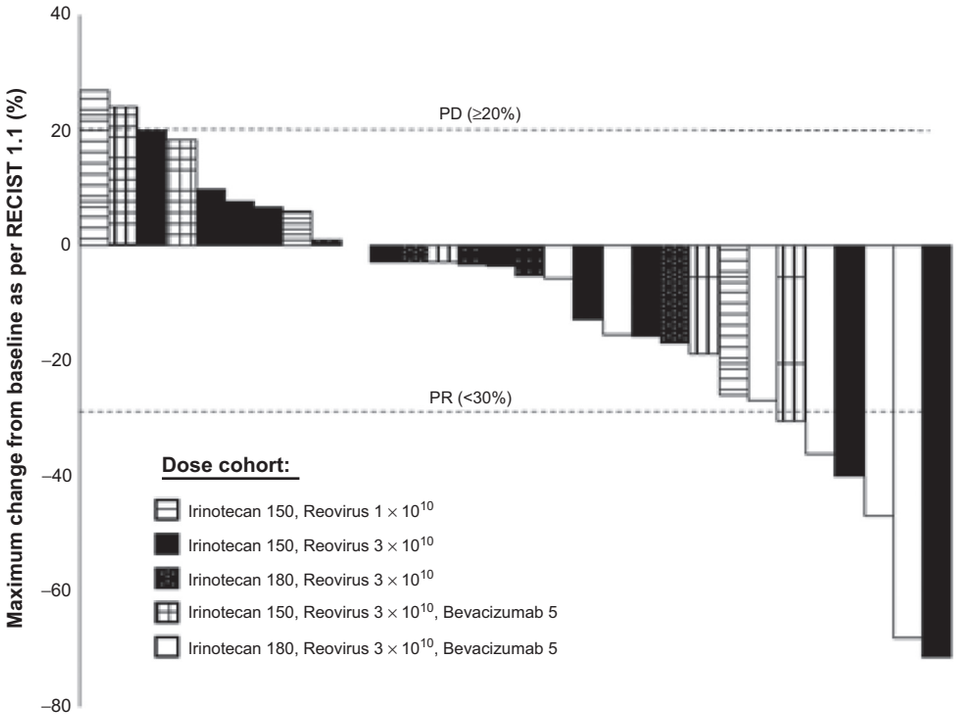

Figure 1.
Waterfall plot of the 30 patients evaluable for tumor response by RECIST 1.1, depicting the best change in overall tumor dimensions. Six patients had a PR as the best response, and 22 had SD.

Patients and Methods

Animal studies

Approval was obtained by the Albert Einstein College of Medicine Institutional Animal Care and Use Committee. Athymic nude mice (Harlan Laboratories # nu69), 8–9 weeks old were injected with 5×10^6 HCT116 cells mixed with Matrigel (1:1) into their right flank, and monitored daily. Drug intervention was begun when tumor volume reached 100 mm^3. Mice were randomized into four groups (12–14 animals each); pelareorep at a daily dose of 10×10^6 tissue culture infective dose-50 ($TCID_{50}$) administered intratumorally, and placebo intraperitoneally, or irinotecan at 1.25 mg/kg body weight twice weekly intraperitoneally and placebo intratumorally, the combination of both active agents, or placebo in both. The animals were monitored for ulceration, bleeding or infection of the skin and tumor, and for decreased mobility or moribund status. The tumor length and width were measured every 72 hours with digital calipers and the tumor volume (width $\times$ length^2) calculated. The animals were euthanized by CO_2 inhalation when the tumor size reached 2,000 mm^3. At the end of 6 weeks, all surviving animals were euthanized, once the final tumor volume measurements were taken. All experiments were performed in triplicate.

Patients and drug administration

This was a three center open-label phase I dose escalation clinical trial. The study enrolled patients between 2011 and 2017 with mCRC who had progressed on or were intolerant to prior oxaliplatin-based therapy in the metastatic setting, or relapsed within 6 months of adjuvant oxaliplatin. Patients were adults ≥18 years; with a pathologic diagnosis of *KRAS*-mutated mCRC. They were required to have an Eastern Cooperative Oncology Group (ECOG) performance status (PS) of 0–1, and with measurable or evaluable disease. Prior bevacizumab was permitted. Patients with history of brain metastases were permitted if the tumors were treated and controlled. A washout period of 28 days was required after cessation of prior radiotherapy or chemotherapy or major surgery. Additional active cancer(s) were excluded. All prior toxicities had to have resolved to grade 1 or less. Key laboratory parameters required were absolute neutrophil count ≥1,500/μL, platelets ≥100,000/μL, bilirubin/alanine aminotransferase/aspartate aminotransferase within normal limits, creatinine clearance ≥50 mL/minute, and urine proteinuria < 30 mg% (once bevacizumab was added). Pregnant and breast-feeding women were excluded.

The primary objective was to determine the dose-limiting toxicity (DLT), MTD, and the recommended phase II dose (RPTD). Only cycle 1 toxicities were considered in identifying a DLT. The latter was defined as a grade ≥3 nonhematologic toxicity (except suboptimally treated nausea/vomiting/diarrhea), grade 4 thrombocytopenia, or grade 3 thrombocytopenia with bleeding, grade 4 neutropenia ≥5 days, and grade ≥3 febrile neutropenia. Use of growth factors was not allowed in the first two cycles. Secondary objectives included pharmacokinetics, pharmacodynamics, immunologic response, and clinical efficacy.

Patients received escalating doses of irinotecan in the FOLFIRI regimen (irinotecan 150–180 mg/m^2 i.v. over 90 minutes, leucovorin 400 mg/m^2 i.v. over 2 hours, followed by 5-FU 400 mg/m^2 bolus, and 5-FU 2,400 mg/m^2 continuous i.v. over 46 hours) and repeated every 14 days. Standard drug preparation and administration guidelines, including antiemetic and atropine premeditations were followed. Pelareorep was supplied by Oncolytics Inc. in vials containing 7.2×10^{11} tissue culture infective dose ($TCID_{50}$) per mL of pelareorep in a phosphate-buffered solution and stored at −70°C. Escalating doses of pelareorep ranging from 1×10^{10} to 3×10^{10} $TCID_{50}$ were administered intravenously over 1 hour on days 1–5 every 28 days (with alternate doses of FOLFIRI chemotherapy).

Prior irinotecan was permitted, until DLTs were observed in 2 patients at the highest irinotecan dose of 180 mg/m^2. The protocol was amended to exclude prior irinotecan chemotherapy exposure.

Furthermore, as clinical data and practice evolved with the survival benefit of continuing bevacizumab (16), it was added to the FOLFIRI regimen. Pelareorep was also moved from cycle 1 to cycle 2, to allow for distinction of FOLFIRI-related from FOLFIRI/pelareorep-related toxicities. The study protocol was approved by all local institutional review boards and ethics committees. All procedures were performed after obtaining such approval. All patients gave written informed consent prior to any study related procedure.

Assessments

Pretreatment evaluation included medical history, physical examination laboratory analyses (CBC, basic metabolic panel, liver function tests, coagulation tests, and urine for proteinuria), within 14 days of first dose. All patients had evaluable disease documented by imaging, including a CT scan of chest, and CT or MRI of abdomen, and pelvis. All laboratory tests were repeated at each treatment cycle, while imaging studies were repeated at 8 weeks, irrespective of dose delays or skipped doses. Response was assessed according to RECIST version 1.1 (17). Patients remained on study until documented progression or intolerable toxicities or patient choice. They were followed every 8 weeks for survival, until death or withdrawal of consent. As there was no expectation of drug–drug interaction, and to minimize patient discomfort and blood draws, limited pharmacokinetic sampling was performed for irinotecan, SN-38, and 5-FU in cycles 1 and 2, both with and without pelareorep (18). Plasma samples were drawn at 0 minute and 90 minutes, and 4 hours, 24 hours, and 48 hours from time of start of irinotecan. The collection and analysis of samples have been previously described by our group (19).

Flow cytometry (FACS)

We also sought to assess the immune-modulating effects of pelareorep, once the MTD was established. Blood was drawn into cell preparation tubes (CPT; BD Vacutainer CPT, Mononuclear Cell Preparation Tubes; manufacturer # 362753) to isolate peripheral blood mononuclear cells (PBMC) at 0, 3, 24, 48, 72, and 96 hours, and 8 and 15 days post day 1 of pelareorep containing and nonpelareorep cycles. FACS assay was performed using fluorophore-labeled antibody staining for Th lymphocyte (FITC-CD4; catalog no. 11-0049; Thermo Fisher Scientific-eBioscience), cytotoxic T lymphocyte (PE-CD8; catalog no. 12-0088; Thermo Fisher Scientific-eBioscience), activated cytotoxic T lymphocyte (CD70-eFluor 660; catalog no. 50-0709; Thermo Fisher Scientific-eBioscience), mature dendritic cell (CD123-PE-Cy7; catalog no. 25-1239; Thermo Fisher Scientific-eBioscience), and Natural killer (NK) cells (CD56-eFluor 450 catalog no. 48-0566; Thermo Fisher Scientific-eBioscience) along with live dead marker(FVD-eFluor 780; catalog no. 65-0865 Thermo Fisher Scientific-eBioscience). The staining and data acquisition were performed within 3 hours of sample collection. FlowJo Software (version 9.8.1) was used for all analysis and gating was maintained unaltered throughout the entire analysis.

Analysis of tumor tissue

Pretreatment tissue, if available, was subjected to molecular analysis by next-generation sequencing (NGS) using the platform by Foundation One. On-study tumor biopsies were optional and were performed on consenting patients. These were analyzed by electron microscopy and IHC.

Transmission electron microscopy

The biopsy samples were fixed with 2% paraformaldehyde and 2.5% glutaraldehyde in 0.1 mol/L sodium cacodylate buffer, post-fixed with 1% osmium tetroxide followed by 1% uranyl acetate, dehydrated through a graded series of ethanol and embedded in LX112 Resin (LADD Research Industries). Ultrathin (80 nm) sections were cut on a Reichert Ultra-cut UCT, stained with uranyl acetate followed by lead citrate. For the immunogold staining, sections were etched with saturated sodium metaperiodate for 1 hour, followed by preheated 0.01 mol/L sodium citrate buffer, pH of 6.0 for 10 minutes, with intermittent microwave heating. Sections were washed with PBS, blocked with 1%BSA, and incubated with primary antibody to viral capsid σ-1 protein (sourced from Oncolytics) overnight at 4°C followed by goat anti-rabbit 10 nmol/L gold particles (https://aurion.nl/) attached secondary antibody for 3 hours at room temperature. Sections were stained with uranyl acetate. All electron microscope images were viewed on a JEOL 1200EX transmission electron microscope at 80 kv.

Statistical analysis

The study followed a standard 3+3 dose escalation design. Once the protocol defined highest dose was reached, a total of 6 patients were enrolled, to confirm safety and tolerability. Descriptive statistics were used to characterize patient demographics, response, and toxicity (including laboratory abnormalities) rates. Time-to-event parameters were analyzed according to the Kaplan–Meier method. GraphPad Prism version 7.0 (GraphPad Software) was used for all statistical analyses.

Table 1. Baseline characteristics ($n = 36$).

Age in years: median (range)	59 (30–77)
Sex	
Female	23 (64%)
Male	13 (36%)
Race	
Non-Hispanic White	19 (53%)
Non-Hispanic Black	12 (33%)
Hispanic	4 (11%)
Asian	1 (3%)
ECOG PS	
0	3 (8%)
1	32 (89%)
2	1 (3%)
Prior treatment	
Surgery	32 (89%)
Chemotherapy	36 (100%)
(FOLFIRI)	13 (37%)
Bevacizumab	9 (25%)
Radiotherapy	13 (37%)
Primary site	
Right colon	10 (28%)
Left colon	15 (42%)
Rectal	11 (30)
Kras mutation status	
G12V	12 (33%)
G12D	10 (28%)
G12C	4 (11%)
G12A	2 (6%)
G13D	2 (6%)
G12'X'	3 (8%)
G12R	1 (3%)
Q61'X'	1 (3%)
K117N	1 (3%)

Note: This table highlights the important clinical characteristics of all the patients who consented and were enrolled in the clinical trial.
Abbreviation: X, unknown/not reported.

Table 2. Treatment-related (possible, probable, or definite) toxicities that occurred in >10% of patients.

Toxicity	Cohort 1			Cohort 2			Cohort 3				Cohort 4			Cohort 5		
Irinotecan	150 mg/m^2			150 mg/m^2			180 mg/m^2				150 mg/m^2			180 mg/m^2		
Pelareorep	1 × 10^{10} TCID$_{50}$			3 × 10^{10} TCID$_{50}$			3 × 10^{10} TCID$_{50}$				3 × 10^{10} TCID$_{50}$			3 × 10^{10} TCID$_{50}$		
Bevacizumab	None			None			None				5 mg/kg			5 mg/kg		
n	3			12			6				7			8		
Grade	2	3	4	2	3	4	2	3	4	5	2	3	4	2	3	4
Myelosuppression																
Neutropenia		1			5	1		1	3			3	1	3	3	
Anemia				3	1		1	2	1			2			3	
Thrombocytopenia				1	1			3	1[a]					1		
Infection				2	1					1[a]				1		
GI symptoms																
Diarrhea				4			2				1	1		3	2	
Constipation	1			1										2		
Nausea	1			2				1			2					
Vomiting				2				1				1	2	1		
Stomatitis[b]					1									1		
Anorexia	1			2							2			1		
Dehydration								1								
Flu-like symptoms																
Fatigue	2			5	2		3				3			3	2	
Pyrexia				1			1							1		
Dehydration								1								
Musculoskeletal[c]					2						4			1		
Generalized																
Dizziness				3							2					
Insomnia				4			2				1			2		
Dyspnea								1						1		
DVT				1							1				2	
HTN				1			1				1			1	3	
Epistaxis				1						1	1			3	1	
Proteinuria											2			3	2	

Note: Summary of all grades (2–5) toxicities observed in >10% of patients that were considered possibly, probably, or definitely related to study related intervention.
[a]DLT.
[b]Includes oropharyngeal pain and mucositis.
[c]Includes arthralgias, back pain, myalgias, extremity pain, and headaches.

Results

Human-derived cell line xenograft study

Twelve to 14 mice were treated in each of the four conditions. We observed a rapid tumor growth in the control mice, and all control mice were sacrificed before 10 days from start of drug intervention. As single agents, irinotecan and pelareorep exhibited a similar degree of tumor growth control (52% and 60%). The mice that received both drugs clearly had the best outcome, with some mice showing complete tumor regressions ($P = 0.0005$). The mean tumor volume reduction in the combination group was 77%, 52%, and 42% compared with control, irinotecan-, and pelareorep-injected tumors, respectively. All mice were sacrificed and euthanized when the tumor volume reached 2,000 mm^3 or at the end of the experiment at 6 weeks (Supplementary Fig. S1).

Patient characteristics

The study enrolled 36 patients with a median age of 59 (range 30–77) years, of which 23 (64%) were women (**Table 1**). All patients had received prior oxaliplatin chemotherapy, and except one, all patients received it in the metastatic setting, and all had progression of disease as the reason for discontinuation. Thirteen (41%) had prior radiotherapy and 13 (41%) had prior FOLFIRI chemotherapy. Seventy percent had colonic, while the other 30% had rectal primary tumors. More than half the patients had either a G12V or a G12D mutation (exon 2, codon 12, *KRAS* gene). At the RPTD, 2 patients withdrew from study after the first dose of FOLFIRI/bevacizumab, did not receive pelareorep, and were not evaluable for toxicity. An additional 4 patients did not receive the planned four cycles of chemotherapy prior to their first disease assessment, due to toxicity or patient choice, leading to 30 patients assessable for response.

Safety, DLTs, MTD, and RPTD

Table 2 lists the grade ≥ 2 toxicities experienced by all the patients in the trial. The initial design of the trial permitted entry of patients with prior irinotecan treatment. Among them, at the irinotecan dose of 180 mg/m^2 (cohort 3), 2 of 6 patients experienced a DLT; 1 patient experienced grade 4 thrombocytopenia, and another developed febrile neutropenia and urosepsis. The latter patient was a 65-year-old male with colon cancer with extensive liver metastases, who had been treated with both FOLFOX and FOLFIRI, both with bevacizumab. He suffered a significant myelosuppressive episode with the first dose of FOLFIRI/pelareorep, developed urosepsis, and finally succumbed to it. This dose was considered to have exceeded the MTD, and the next lower dose cohort of irinotecan at 150 mg/m^2 (cohort 2), was tested and was well tolerated, with no DLT observed among the 12 patients treated. At this time, the protocol was amended to include

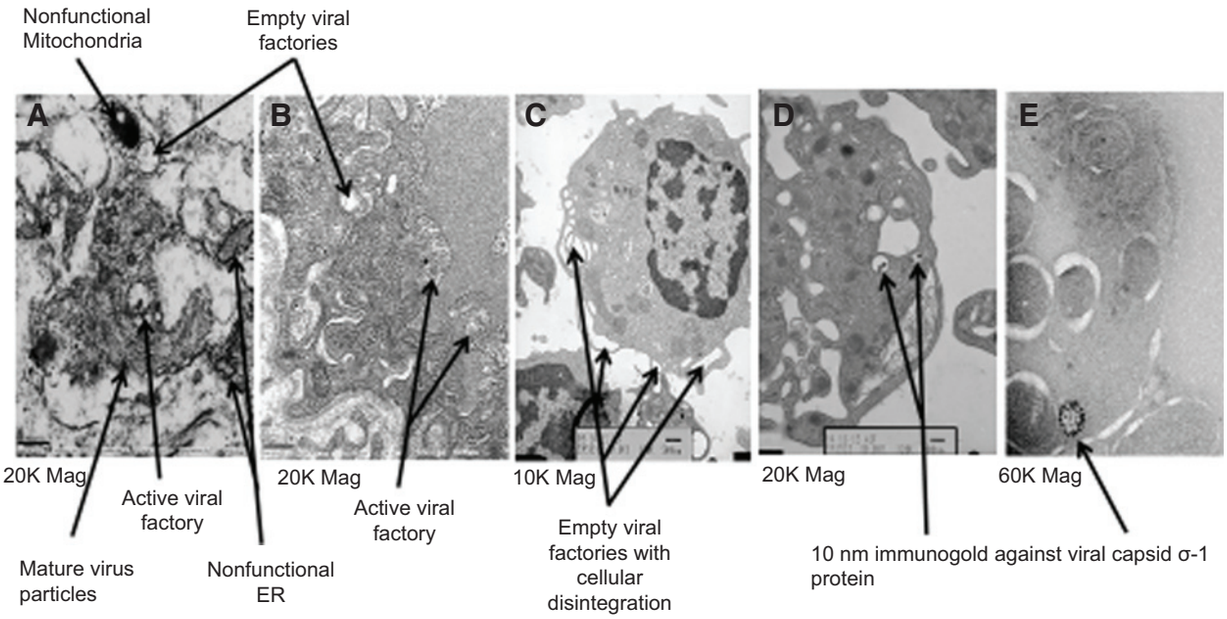

Figure 2.

This figure depicts the key findings from electron micrographs representing the process of virus propagation. **A,** Empty and active viral factories as well as nonfunctional subcellular organelles including mitochondria and endoplasmic reticulum confirming that the cell is dying. **B,** Several active viral factories. **C,** The process of cellular disintegration at points of empty viral factories. **D** and **E,** Immunogold staining of the tumor sample obtained by biopsy of a patient using 10-nm gold particles to detect the localization of pelareorep sigma 1 capsid protein again seen confined to viral factories (magnification, 60×).

bevacizumab, and to exclude prior FOLFIRI (cohorts 4–5). No further DLT was observed, and cohort 5 was declared the RPTD, full dose of FOLFIRI (irinotecan at 180 mg/m^2, every 14 days), and the highest single-agent dose of pelareorep (3×10^{10} $TCID_{50}$ on days 1–5 every 28 days).

The most common grade ≥2 toxicities experienced by the patients can be grouped into three groups, including myelosuppression [neutropenia, $n = 21$ (58%; (grade ≥3, 50%)); and anemia, $n = 13$ (36%; (grade ≥3, 25%))]; gastrointestinal [diarrhea ($n = 13$ (36%; (grade ≥ 3, 8%))]; and constitutional [fatigue, $n = 20$ (36%; (grade ≥3, 11%)}]. Fever was observed in 3 patients, clearly attributable to the pelareorep administration, similar to prior experience (20). Two patients suffered from grade 3 proteinuria, attributable to the bevacizumab. No overlapping toxicities of concern were observed in this study.

Response and clinical benefit

All patients underwent imaging every 8 weeks, irrespective of dose delays or skipping of therapy. Images were reviewed by an independent radiologist, and response assessed as per RECIST 1.1 (17). At the RPTD, 3 of 6 patients experienced a partial response (PR; **Fig. 1**). Overall, of the 30 evaluable patients, 6 (20%) had a PR, and 22 patients (73.3%) had stable disease (SD) as their best response, with a clinical benefit rate (PR + SD) of 93.3%. Among the 6 patients with a PR, 4 had liver only metastases, 1 had metastases in lung, liver, and abdominal masses, and the sixth patient had pelvic masses and lymph nodes (Supplementary Table S1). Two patients had progression of disease at their first post-therapy initiation imaging. The median progression free survival (PFS) was 65.6 weeks at the RPTD, and 22.2 weeks for all patients. The OS was 25.1 months at the RPTD, and 11.7 months for all patients (Supplementary Fig. S1). Of note, 1 patient had to discontinue the study due to inability to keep up with the 5 days of pelareorep administration, and was continued on FOLFIRI/bevacizumab. Encouragingly, she stayed on this regimen for 19.5 additional months after withdrawal of study, until she experienced disease progression.

Across all doses, 13 patients were treated with FOLFIRI prior to study entry and their PFS and OS was 18.5 weeks and 9.7 months, respectively. In contrast, among patients who were FOLFIRI naïve, the PFS and OS was 25.7 weeks and 19.5 months, respectively. Not surprisingly, the clinical outcome was numerically better for patients that were FOLFIRI naïve; however, this study was clearly not designed for studying this question.

Pharmacokinetics

Consistent with our expectation, there was no evidence of any pharmacokinetic drug–drug interaction between pelareorep and chemotherapy (Supplementary Table S1). As expected, the mean AUC (exposure) of irinotecan was higher at the 180 mg/m^2 cohort than the 150 mg/m^2. There was no discernible difference in the AUC, or clearance in the presence or absence of pelareorep. Similarly, no differences were observed in the pharmacokinetic of SN-38 or 5-FU.

In depth analysis of tumor mutations

All 36 enrolled patients carried a mutation in *KRAS* (details in **Table 1**). Among them, 22 had available tissue that was assayed by NGS. In addition, 1 patient's tissue was assayed for BRAF mutations. Of the 22 patients, 8 had a mutation in the PI3K pathway, with a mutation in PIK3CA or PTEN. As expected, 18 of the 22 had an APC mutation and 10 had a p53 mutation. Among the 23 patients in whom the BRAF status was known, only 1 had a mutation. This lower rate of BRAF mutations is consistent with prior observations that there is almost a "mutual exclusivity" or RAS and BRAF mutations (Supplementary Table S1).

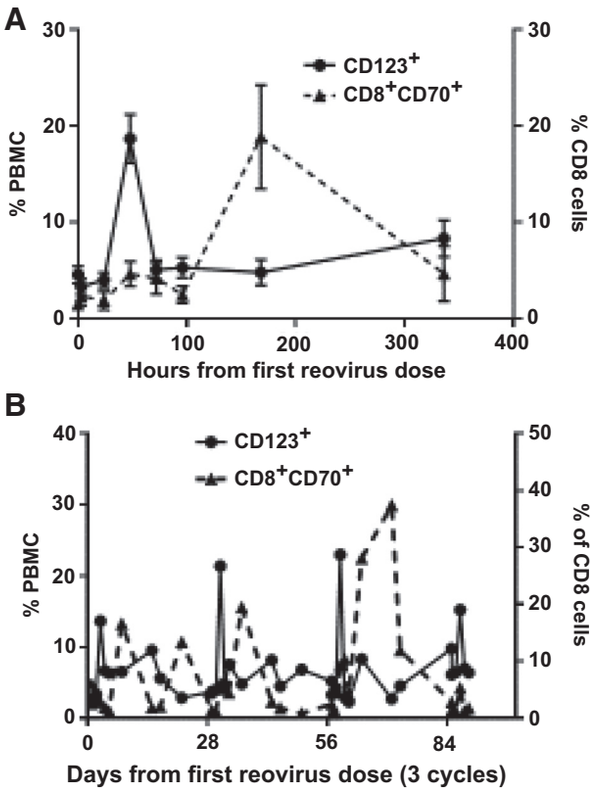

Figure 3.

A, FACS analysis of changes in circulating immune cells. Samples were collected from 5 patients treated at the RPTD over 14 cycles. The graphs depict mean and SEM. A rapid peak of the dendritic cell maturation was observed at 48 hours, followed by the activation of CD8 T cells at 7 days. **B,** FACS analysis of changes in circulating immune cells from a single patient at the RPTD over 3 cycles. In each cycle, samples were drawn on days 1, 3, 8, 15, 17, and 29 (day 1 of next cycle), and ended on day 85 (day 1 of cycle 4). A peak in the dendritic cell maturation was observed at 48 hours (days 3, 31, 59, and 87), followed by activation of CD8 T cells after 7 days (days 8, 36, and 64), a process repeated with a dose of pelareorep delivered every 28 days.

Pharmacodynamics

On study biopsies were obtained from 3 patients, of which 1 was subject to NGS, 1 to transmission electron microscopy (TEM) and IHC staining, and the third for both studies. TEM showed distinct morphology relating to pelareorep growth and propagation. The viruses home themselves into a vesicular structure indicated as viral factories (**Fig. 3A** and **B**), where new virions assemble [**Fig. 2A**, B, and D (immunogold staining)]. At a magnification of 20,000 ×, in the cells containing viral factories, the nonfunctional endoplasmic reticulum, mitochondria, and the mature viral particles are evident. Upon dissemination of virus, the empty factories disintegrate causing overall cytoplasmic disintegration. This is clear at a lower magnification of 10,000 × (**Fig. 3C**). The presence of multiple viral factories engaged at various stages of virus development in a single-tumor cell (**Fig. 3A–C**) indicates simultaneous infection by several viruses. The tumor cell nucleus has sufficient euchromatin regions supporting the notion that transcription is active within the cell while virus-mediated cytoplasmic degeneration is in progress (**Fig. 3C**). Another distinct cytoplasmic feature is the presence of multivesicular bodies indicating that the cell is in distress. As further evidence of viral homing into the tumor, we detected the viral particles embedded within tumor cells, using immune gold staining for the pelareorep capsid σ-1 protein (**Fig. 3D**).

With regard to NGS assay, 1 patient had a *KRAS G12D, APC R1450*, IDH1R132C*, both in the pre- and post-pelareorep sample, but gained a *PIK3CA* R357Q mutation in the post-pelareorep sample. The second patient had a *KRAS* G12V and *SMAD4 G419R* mutation on the pre- and *KRAS* G12V, *ERRFI1* loss, *APC* Y622fs*7, *ARID1A* Q1584*, *DNMT3A* R882H (subclonal) on the post-pelareorep specimen. With this limited dataset, it appears that the nature of the *KRAS* mutation remains intact with pelareorep therapy.

Immune response

We performed an in depth study using FACS to isolate and quantify lymphocytes from PBMC at the RPTD. Among the 6 patients entered, 5 consented to PBMC sampling for FACS. Samples were collected at protocol specified times points in one cycle in 1 patient, and in multiple cycles in 4 patients.

A very rapid maturation of the dendritic cells was observed at 48 hours, from a baseline mean of 4.5% to a mean of 18.6% (4.1-fold change, $P = 0.000016$). This was followed by an increase in absolute CD8 counts (2.4-fold change, $P = 000015$), and CD4 counts (3.5-fold change, $P = 000015$), on day 4. The most important observation was the activation of CD8 cells ($CD8^+CD70^+$) on day 8, from a baseline mean of 1.5% to a mean of 18.8% (12.9-fold change, $P = 0.0009$; **Fig. 3A**). A simultaneous drop in nonactivated CD8 cells ($CD8^+$ $CD70^-$) accompanied this increase in activated CD8 cells. Samples were also drawn at 48 hours and 7 days post-FOLFIRI chemotherapy infused without pelareorep. Not surprisingly, a similar dendritic cell maturation and CD8 activation were not replicated. This unique pattern of dendritic cell maturation followed by CD8 activation was observed repeatedly with each dose of pelareorep (representative patient data shown in **Fig. 3B**). The details of the change in CD8 and CD70 cells in a representative patient are shown in **Fig. 4**. We did not observe any obvious common pattern of the NK cells in response to pelareorep.

Discussion

The idea of using viruses to target cancer dates back to over a century (21). More recently, there has been a renewed interest in the use of infectious agents, such as viruses, as adjuncts in the treatment of cancer. Single agent use of pelareorep has been supplanted by convincing preclinical and clinical evidence that chemotherapy facilitates better delivery of pelareorep into the tumor (15, 22–24). Pelareorep has been tested in multiple clinical trials to date, both, as an intratumoral injection, and intravenously (15). These trials have each demonstrated unique toxicities depending on the cytotoxic agent employed (25, 26). These unique findings highlight the need to conduct careful well-planned phase I combination dose escalation studies, when studying two agents with widely differing mechanisms of action.

Over the past decade, an oncogenic mutation in *KRAS* in a patient's tumor with mCRC is entrenched as a biomarker of exclusion of anti-EGFR therapy (3, 27). The urgent need for novel approaches for this specific patient population cannot be overemphasized. Our group has previously proven synergistic anticancer activity using *in vitro* model systems of the combination of pelareorep with irinotecan (12). We demonstrated that pelareorep preferentially induced apoptosis in the *KRAS* mutant rather than *KRAS* WT genotype in a panel of colorectal cancer cell lines.

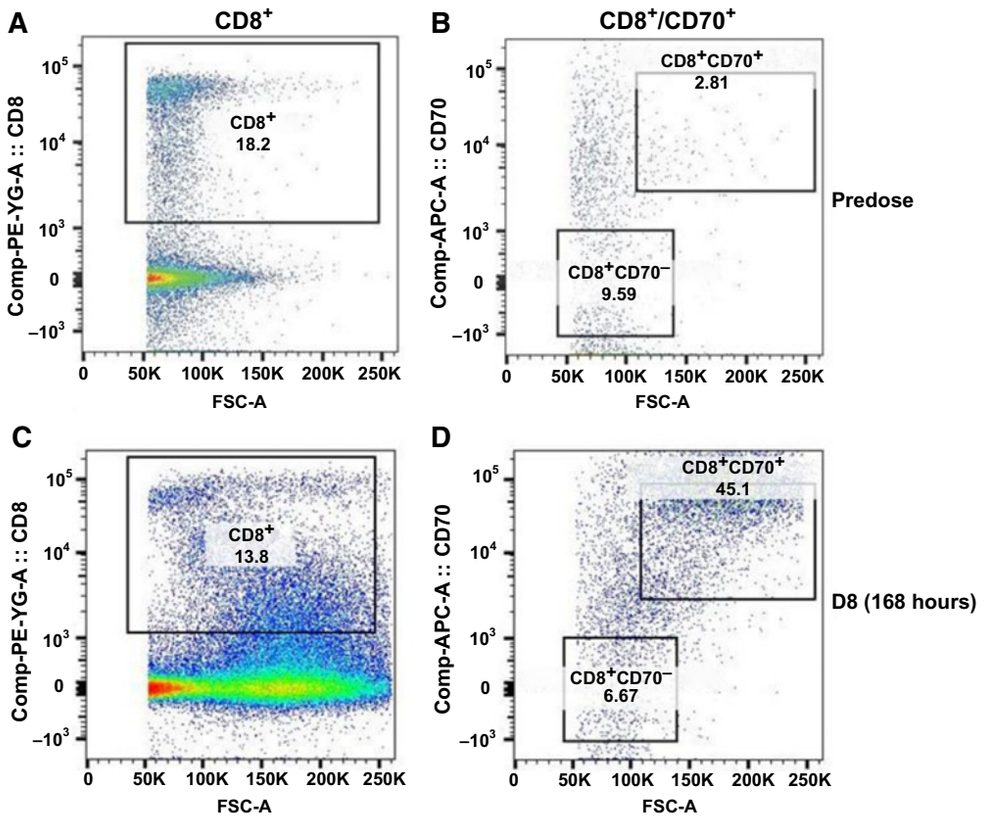

Figure 4.

A–D, Flow cytometry analysis of bivariate ($CD8^+$ $CD70^+$) cell population in a representative patient's PBMC at pre (day 1 prior to pelareorep administration) and day 8 (D8, 168 hours post dose). Cells were labeled with PE-CD8 (eBioscience #12-0088-80) and efluro660-CD70 (eBioscience # 50-0709) antibodies post-live dead (FVD eFluro780 # 65-0865) staining. The $CD8^+$ cell population was gated out of the live cell population. The $CD8^+$ cells were further selected for $CD8^+CD70^+$ and $CD8^+CD70^-$ population (indicated in square boxes). The $CD8^+$ cell population with low CD70 expression was carefully excluded from the analysis. The D8 $CD8CD70^+$ population increased from 2.8% to 45.1%.

In this multi-center, biomarker driven, phase I study, the combination of FOLFIRI/bevacizumab chemotherapy with pelareorep was well tolerated; the highest doses of each individual drug was easily deliverable; strong efficacy signals were observed at the RPTD; and correlative science demonstrated a unique immune enhancing phenomenon, and electron microscopic characteristics. No DLT was observed in the first 28 days of assessment. The only DLT events observed were in the patients with prior exposure to FOLFIRI therapy, and were related to myelosuppression, attributable to the chemotherapy component of the regimen, rather than the pelareorep. Overall, grade 3–5 neutropenia was seen in 18 (50%) patients, which is higher than previously seen with FOLFIRI/anti-VEGF agent combination studies (16, 28, 29); however, this may be explained by cumulative neutropenia from the prolonged therapy. Grade 3–4 diarrhea was experienced by 8% of patients, similar to historical data.

Recent progress in second-line therapy for mCRC has included three anti-VEGF agents, bevacizumab (16), aflibercept (28), and ramucirumab (29), improving OS by 1.4–1.6 months compared with FOLFIRI, to a median of 11.2–13.5 months. In comparison, in this study, at the RPTD, the median PFS of the 6 patients was 65.6 weeks, and median OS was 25.1 months. Such a dramatic improvement compared with historic data is encouraging, warranting further testing. Anecdotally, 1 patient withdrew consent as she was not able to keep up with the rigorous schedule of pelareorep administration, and continued on FOLFIRI/bevacizumab alone, well beyond 19 months.

This is not the first time that pelareorep underwent evaluation in mCRC. In a separate randomized phase II study in first-line patients; it was combined with standard FOLFOX chemotherapy (30). The primary endpoint was PFS, and surprisingly the pelareorep arm was inferior, although the response rates were higher, and OS did not differ. In a randomized phase II study in men with castrate-resistant prostate cancer, patients received docetaxel/prednisone with or without pelareorep (31). Overall, the study had no efficacy improvement observed. Although the 12 week "lack of progression" was improved with pelareorep, the median OS was not different. These two studies highlight the difficulty of translating preclinical science into clinical results. There is no data on the combination of pelareorep and oxaliplatin specifically in colorectal cancer models, and on the combination of pelareorep and docetaxel in prostate cancer models. It is quite well established that preclinical success is no guarantee of clinical success, while preclinical failure or lack of successful data is a sure road to clinical failure. Second, the patients were not selected on the basis of Ras status in either study. The lack of a predictive biomarker may have contributed to the disappointing results too. This study, on the other hand, is built on robust *in vitro* data showing preferential susceptibility

in Ras-mutant conditions, and *in vitro* and *in vivo* data demonstrating synergy with irinotecan.

Correlative science involved detailed FACS-based assays for immune markers. A very rapid maturation of the dendritic cells that are potent antigen-presenting cells was observed at 48 hours, and subsequently, a peak in the CD8 activation was seen after 7 days. This significant activation of the host adaptive immune system is a likely contributor to the efficacy of the pelareorep. More importantly, such dendritic cell maturation and activation of CD8 was observed with every cycle of pelareorep dosing, suggesting that the host immune response (neutralizing anti-pelareorep antibody, NARA) was insufficient in suppressing viral replication, allowing for sustained clinical benefit. It is well established that NARA is detectable in patients prior to first dose of pelareorep, and its titer increases by hundreds of fold upon exposure to pelareorep (20, 32). On the same theme, a prior report argued that pelareorep is carried within dendritic cells, and able to evade host immunity (33).

Our electron microscopy findings are consistent with the fact that that the virus exerts dual mode of tumor cell killing. While being a potent immune stimulator it also physically destroys the tumor cells by forming active viral factories. In such events, the subcellular organelles like mitochondria and rough endoplasmic reticulum lose structural architecture, and several multicellular bodies are formed indicating progression toward cellular death. Interestingly the obvious chromosomal condensation is not observed until the very end, probably because the virus controls the transcriptional activities and continues to help maximize the synthesis of active virions. Perhaps for the first time, we have elucidated, by electron microscopy, the chronology of the intracellular morphologic changes in the structure and organelles taking place because of pelareorep infection.

The further development of pelareorep could take many shapes and forms. One interesting approach under study is the utilization of viruses to convert "cold" tumors into "hot" or "inflamed" tumors. With the advent of immunotherapy, there is tremendous interest in combining viruses with immune checkpoint inhibitors (34–37). Early results from *in vivo* models of syngeneic mice from our laboratory have shown synergistic activity with anti-mouse PD-1 mAb specifically in *KRAS*-mutant microsatellite stable (MSS) colorectal cancer, but not so in *KRAS* WT microsatellite unstable mice (36). Specifically, the combination of pelareorep and checkpoint inhibitor has been studied in patients with pancreatic ductal adenocarcinoma, with encouraging signs of activity (37). This is of particular interest in the patients with tumors harboring a *KRAS* mutation that tend to have a higher prevalence of MSS tumors (2).

Disclosure of Potential Conflicts of Interest

S. Goel reports receiving a commercial research grant from Oncolytics Inc. A.J. Ocean is a consultant (paid consultant) at Celgene and Tyme Therapeutics, Inc., is an advisory board member at Agios and Array, and has received speakers bureau honoraria from Daiichi Sanyko. M. Coffey is president, CEO (paid consultant) at, has ownership interest (including patents) in, and has provided expert testimony for Oncolytics Biotech Inc. No potential conflicts of interest were disclosed by the other authors.

Authors' Contributions

Conception and design: S. Goel, M. Coffey, R. Maitra
Development of methodology: S. Goel
Acquisition of data (provided animals, acquired and managed patients, provided facilities, etc.): S. Goel, A.J. Ocean, R.Y. Parakrama, M.H. Ghalib, I. Chaudhary, U. Shah, R. Maitra
Analysis and interpretation of data (e.g., statistical analysis, biostatistics, computational analysis): S. Goel, A.J. Ocean, M.H. Ghalib, I. Chaudhary, M. Coffey, R. Maitra
Writing, review, and/or revision of the manuscript: S. Goel, M.H. Ghalib, I. Chaudhary, S. Viswanathan, H. Kharkwal, M. Coffey, R. Maitra
Administrative, technical, or material support (i.e., reporting or organizing data, constructing databases): S. Goel, I. Chaudhary, S. Viswanathan, H. Kharkwal
Study supervision: S. Goel

Acknowledgments

The authors deeply appreciate the willingness of the patients to participate in the trial and to their families who supported them all along. This study would not have been possible without such contribution. We further want to extend our sincere thanks to Dr. Lydia Tesfa, ex-Associate Director, Flow Cytometry core facility and Ms. Leslie Gunther-Cummins, Electron Microscope Specialist, Analytical Imaging Facility of Albert Einstein College of Medicine (Bronx, NY) for their constant support and guidance throughout the execution of the project.

The costs of publication of this article were defrayed in part by the payment of page charges. This article must therefore be hereby marked *advertisement* in accordance with 18 U.S.C. Section 1734 solely to indicate this fact.

Received December 3, 2019; revised February 4, 2020; accepted March 5, 2020; published first March 10, 2020.

References

1. Allegra CJ, Jessup JM, Somerfield MR, Hamilton SR, Hammond EH, Hayes DF, et al. American Society of Clinical Oncology provisional clinical opinion: testing for KRAS gene mutations in patients with metastatic colorectal carcinoma to predict response to anti-epidermal growth factor receptor monoclonal antibody therapy. J Clin Oncol 2009;27:2091–6.
2. Cancer Genome Atlas Network Comprehensive molecular characterization of human colon and rectal cancer. Nature 2012;487:330–7.
3. National Comprehensive Cancer Network. https://www.nccn.org/professionals/physician_gls/pdf/colon.pdf. Accessed July 16, 2019.
4. Goldberg RM, Rothenberg ML, Van Cutsem E, Benson AB III, Blanke CD, Diasio RB, et al. The continuum of care: a paradigm for the management of metastatic colorectal cancer. Oncologist 2007;12:38–50.
5. Aparo S, Goel S. Evolvement of the treatment paradigm for metastatic colon cancer. From chemotherapy to targeted therapy. Crit Rev Oncol Hematol 2012;83:47–58.
6. Merla A, Goel S. Novel drugs targeting the epidermal growth factor receptor and its downstream pathways in the treatment of colorectal cancer: a systematic review. Chemother Res Pract 2012;2012:387172.
7. Porru M, Pompili L, Caruso C, Biroccio A, Leonetti C. Targeting KRAS in metastatic colorectal cancer: current strategies and emerging opportunities. J Exp Clin Cancer Res 2018;37:57.
8. McCormick F. Targeting KRAS directly. Annu Rev Cancer Biol 2018;2:81–90.
9. Grothey A, Cutsem EV, Sobrero A, Siena S, Falcone A, Ychou M, et al. Regorafenib monotherapy for previously treated metastatic colorectal cancer (CORRECT): an international, multicentre, randomised, placebo-controlled, phase 3 trial. The Lancet 2013;381:303–12.
10. Mayer RJ, Van Cutsem E, Falcone A, Yoshino T, Garcia-Carbonero R, Mizunuma N, et al. Randomized trial of TAS-102 for refractory metastatic colorectal cancer. N Engl J Med 2015;372:1909–19.
11. Coffey MC, Strong JE, Forsyth PA, Lee PW. Reovirus therapy of tumors with activated Ras pathway. Science 1998;282:1332–4.
12. Maitra R, Seetharam R, Tesfa L, Augustine TA, Klampfer L, Coffey MC, et al. Oncolytic reovirus preferentially induces apoptosis in KRAS mutant colorectal cancer cells, and synergizes with irinotecan. Oncotarget 2014;5:2807–19.
13. Strong JE, Lee PW. The v-erbB oncogene confers enhanced cellular susceptibility to reovirus infection. J Virol 1996;70:612–6.
14. Strong JE CM, Tang D, Sabinin P, Lee PW. The molecular basis of viral oncolysis: usurpation of the Ras signaling pathway by reovirus. EMBO J 1998;17:3351–62.
15. Maitra R, Ghalib MH, Goel S. Reovirus: a targeted therapeutic–progress and potential. Mol Cancer Res 2012;10:1514–25.

16. Bennouna J, Sastre J, Arnold D, Österlund P, Greil R, Van Cutsem E, et al. Continuation of bevacizumab after first progression in metastatic colorectal cancer (ML18147): a randomised phase 3 trial. Lancet Oncol 2013;14:29–37.
17. Eisenhauer EA, Therasse P, Bogaerts J, Schwartz LH, Sargent D, Ford R, et al. New response evaluation criteria in solid tumours: revised RECIST guideline (version 1.1). Eur J Cancer 2009;45:228–47.
18. Mick R, Gupta E, Vokes EE, Ratain MJ. Limited-sampling models for irinotecan pharmacokinetics-pharmacodynamics: prediction of biliary index and intestinal toxicity. J Clin Oncol 1996;14:2012–9.
19. Goel S, Desai K, Karri S, Gollamudi R, Chaudhary I, Bulgaru A, et al. Pharmacokinetic and safety study of weekly irinotecan and oral capecitabine in patients with advanced solid cancers. Invest New Drugs 2007;25:237–45.
20. Gollamudi R, Ghalib MH, Desai KK, Chaudhary I, Wong B, Einstein M, et al. Intravenous administration of reolysin, a live replication competent RNA virus is safe in patients with advanced solid tumors. Invest New Drugs 2010;28:641–9.
21. Webb HE, Smith CE. Viruses in the treatment of cancer. Lancet 1970;1:1206–8.
22. Qiao J, Wang H, Kottke T, White C, Twigger K, Diaz RM, et al. Cyclophosphamide facilitates antitumor efficacy against subcutaneous tumors following intravenous delivery of reovirus. Clin Cancer Res 2008;14:259–69.
23. Gong J, Sachdev E, Mita AC, Mita MM. Clinical development of reovirus for cancer therapy: an oncolytic virus with immune-mediated antitumor activity. World J Methodol 2016;6:25–42.
24. Phillips MB, Stuart JD, Rodriguez Stewart RM, Berry JT, Mainou BA, Boehme KW. Current understanding of reovirus oncolysis mechanisms. Oncolytic Virother 2018;7:53–63.
25. Heinemann L, Simpson GR, Boxall A, Kottke T, Relph KL, Vile R, et al. Synergistic effects of oncolytic reovirus and docetaxel chemotherapy in prostate cancer. BMC Cancer 2011;11:221.
26. Lolkema MP, Arkenau HT, Harrington K, Roxburgh P, Morrison R, Roulstone V, et al. A phase I study of the combination of intravenous reovirus type 3 Dearing and gemcitabine in patients with advanced cancer. Clin Cancer Res 2011;17:581–8.
27. Douillard JY, Oliner KS, Siena S, Tabernero J, Burkes R, Barugel M, et al. Panitumumab-FOLFOX4 treatment and RAS mutations in colorectal cancer. N Engl J Med 2013;369:1023–34.
28. Van Cutsem E, Tabernero J, Lakomy R, Prenen H, Prausova J, Macarulla T, et al. Addition of aflibercept to fluorouracil, leucovorin, and irinotecan improves survival in a phase III randomized trial in patients with metastatic colorectal cancer previously treated with an oxaliplatin-based regimen. J Clin Oncol 2012;30:3499–506.
29. Tabernero J, Yoshino T, Cohn AL, Obermannova R, Bodoky G, Garcia-Carbonero R, et al. Ramucirumab versus placebo in combination with second-line FOLFIRI in patients with metastatic colorectal carcinoma that progressed during or after first-line therapy with bevacizumab, oxaliplatin, and a fluoropyrimidine (RAISE): a randomised, double-blind, multicentre, phase 3 study. Lancet Oncol 2015;16:499–508.
30. Jonker DJ, Tang PA, Kennecke H, Welch SA, Cripps MC, Asmis T, et al. A randomized phase II study of FOLFOX6/bevacizumab with or without pelareorep in patients with metastatic colorectal cancer: IND.210, a Canadian Cancer Trials Group Trial. Clin Colorectal Cancer 2018;17:231–9.
31. Eigl BJ, Chi K, Tu D, Hotte SJ, Winquist E, Booth CM, et al. A randomized phase II study of pelareorep and docetaxel or docetaxel alone in men with metastatic castration resistant prostate cancer: CCTG study IND 209. Oncotarget 2018;9:8155–64.
32. Vidal L, Pandha HS, Yap TA, White CL, Twigger K, Vile RG, et al. A phase I study of intravenous oncolytic reovirus type 3 Dearing in patients with advanced cancer. Clin Cancer Res 2008;14:7127–37.
33. Adair RA, Scott KJ, Fraser S, Errington-Mais F, Pandha H, Coffey M, et al. Cytotoxic and immune-mediated killing of human colorectal cancer by reovirus-loaded blood and liver mononuclear cells. Int J Cancer 2013;132:2327–38.
34. Rajani K, Parrish C, Kottke T, Thompson J, Zaidi S, Ilett L, et al. Combination therapy with reovirus and anti-PD-1 blockade controls tumor growth through innate and adaptive immune responses. Mol Ther 2016;24:166–74.
35. Samson A, Scott KJ, Taggart D, West EJ, Wilson E, Nuovo GJ, et al. Intravenous delivery of oncolytic reovirus to brain tumor patients immunologically primes for subsequent checkpoint blockade. Sci Transl Med 2018;10:pii: eaam7577.
36. Augustine TM, Maitra R, John P, Goel S. Potentiating effect of reovirus in anti-PD1 therapy in colorectal cancer. [abstract]. In: Proceedings of the American Association for Cancer Research Annual Meeting 2018; 2018 Apr 14–18; Chicago, IL. Philadelphia (PA): AACR; 2018. Abstract nr 3917.
37. Mahalingam D, Wilkinson GA, Eng KH, Fields P, Raber P, Moseley JL, et al. Pembrolizumab in combination with the oncolytic virus pelareorep and chemotherapy in patients with advanced pancreatic adenocarcinoma: a phase Ib study. Clin Cancer Res 2020;26:71–81.